Tutorial

Danilo De Simone*, Yannick Vesters and Geert Vandenberghe

Photoresists in extreme ultraviolet lithography (EUVL)

DOI 10.1515/aot-2017-0021
Received March 14, 2017; accepted April 19, 2017; previously published online May 19, 2017

Abstract: The evolutionary advances in photosensitive material technology, together with the shortening of the exposure wavelength in the photolithography process, have enabled and driven the transistor scaling dictated by Moore's law for the last 50 years. Today, the shortening wavelength trend continues to improve the chips' performance over time by feature size miniaturization. The next-generation lithography technology for high-volume manufacturing (HVM) is extreme ultraviolet lithography (EUVL), using a light source with a wavelength of 13.5 nm. Here, we provide a brief introduction to EUVL and patterning requirements for sub-0-nm feature sizes from a photomaterial standpoint, discussing traditional and novel photoresists. Emphasis will be put on the novel class of metal-containing resists (MCRs) as well as their challenges from a manufacturing prospective.

Keywords: CAR; EUV photoresists; MCR; metal-containing resist; metal oxide resist.

1 Introduction

Today, in every electronic device, there is a microchip that performs the requested tasks. These devices have seen a continuous increase in their performance together with a notable miniaturization over the past 50 years. This incredible trend, predicted by Moore's law, is possible, thanks to intensive research and development in order to scale down the size of every single transistor in the integrated circuits. The main enabler for this feature size reduction is the lithographic pattern printing process as schematized in Figure 1.

As the current immersion lithography using 193-nm-wavelength light is reaching its limits, the next-generation lithography technology for the high-volume manufacturing, likely to be introduced for the 5-nm node [1], is the extreme ultraviolet lithography (EUVL), using a light source with a wavelength of 13.5 nm. Because of the high material absorbance at this wavelength, EUVL has introduced three fundamental differences with respect to a 193-nm lithography: (i) the use of reflective multilayer (Bragg type) optics instead of refractive optics, (ii) the plasma light source instead of a DUV laser, and (iii) a vacuum environment with high level of contamination control instead of atmospheric pressure as in DUV [2]. The basic elements for an EUV lithographic system are reported in Figure 2.

One issue of EUVL has been the power of the light source and its operation reliability, but advances in engineering [4] today are promising in reaching the target of 250 W and >85% source availability [5]. Another challenge that is imminent concerns the photoresist performance. In fact, in order to have a powerful EUVL platform for advanced manufacturing device, it is important to have a resist meeting the demanding requirements on resolution (R), line edge roughness (LER), and sensitivity (S). The resolution is the smallest feature size that can be printed with adequate control. Minimum critical dimension (CD) between 20 nm and 10 nm for features with a pitch between 40 nm and 20 nm can be achieved with EUVL [6]. The LER for line-space dense features is defined as the deviation (variability) from an ideal smooth shape (viewed top-down) [7]. Sensitivity is defined as the exposure dose required to get a sufficient degree of chemical response in the resist to obtain the desired features after the development process [8]. As the power source is limited and in order to ensure a sufficient throughput of the EUV production scanner tool, the EUV dose at wafer level should be the lowest possible and ideally below 20 mJ/cm^2 [4]. These

***Corresponding author: Danilo De Simone,** Advanced Patterning Department, IMEC, Kapeldreef 75, Heverlee B-3001, Belgium, e-mail: danilo.desimone@imec.be
Yannick Vesters: Advanced Patterning Department, IMEC, Kapeldreef 75, Heverlee B-3001, Belgium; and Department of Chemistry, KU Leuven, Celestijnenlaan 200F, Heverlee B-3001, Belgium
Geert Vandenberghe: Advanced Patterning Department, IMEC, Kapeldreef 75, Heverlee B-3001, Belgium

www.degruyter.com/aot
© 2017 THOSS Media and De Gruyter

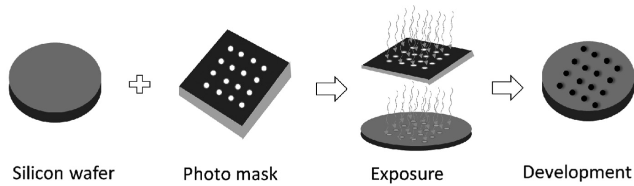

Figure 1: Schematic view of the photolithographic exposure step. The process begins with a clean silicon wafer spin coated with a resist. A mask defines the structures to be printed, and an exposure tool with a mask aligner is used to pass the light through the mask onto the wafer. Exposed resist is washed away during development, while unexposed resist remains.

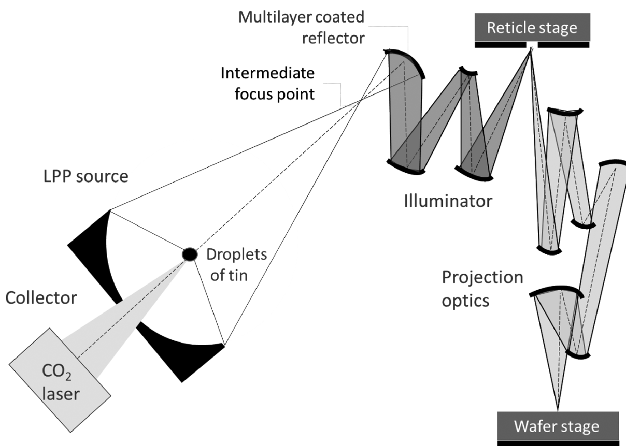

Figure 2: Schematic view of an EUV lithography system [3]. An EUV light source produces 13.5-nm-wavelength light in a system called laser-produced plasma source (LPP). LPP light sources utilize a high power laser to create a high-energy plasma that emits short wavelength light inside a vacuum chamber. In this version, pulses from a CO_2 laser illuminate droplets of tin, which radiate 13.5 nm of light in all directions. A collector mirror focuses the light into a reflective optical system (illuminator) that directs the light onto a reticle (i.e. a mask containing the pattern to be printed). The EUV beam reflected by the reticle is focused by a second set of mirrors (projection optics) onto the wafer stage to print a pattern into a photoresist coated on a wafer surface.

requirements are often called the RLS triangle [9, 10], as trade-off relations between each pair make the simultaneous fulfillment of the three targets extremely challenging. Although the LER can be modulated by augmenting the numerical aperture of the lens (NA) until 0.33 now or 0.55 NA in the future [11, 12] or increasing the aerial image contrast by the use of off-axis illumination (OAI), it has only been slowly and painfully reduced. The resolution is strongly affected by the resist pattern collapse, which becomes increasingly important as feature sizes move into the nm-size range. The pattern collapse mechanism has been intensively studied [13]. It occurs when physical properties of the materials cannot withstand the capillary force during the drying of the rinse liquid [14]. Pattern collapse depends on the pattern height or aspect ratio. The critical aspect ratio, at which patterns begin to collapse, is approximately 2 (for 22-nm features) [15]. However, reducing the resist film thickness induces more challenges on the pattern transfer.

Furthermore, at the nanometer dimensions, stochastic variations during EUVL process influence the variability of the nanoscale patterning. Lithography variability has been shown to be the product of all the lithographic elements: source, mask, optical system, and resist [16]. The specifications required and their control for printing sub-20 nm features are getting closer to the discrete essence of nature of both light and matter. Photon shot noise, mask roughness, and chemical stochastic effects seem insurmountable barriers dictated by physics. Indeed, an important aspect to be considered in the EUVL and resist LER is the photon energy involved in the exposure of photosensitive material and the consequent stochastic effect in the LER. Indeed, with the shortening of exposure wavelength, the photon energy increases from 5 eV at 248 nm wavelength to 6 eV at 193 nm wavelength and then to 91.6 eV at 13.5 nm wavelength. Low exposure dose of high-energy photons causes the number of photons to fall low enough that the statistical variations may be responsible for shot noise and LER [17]. All this puts more stringent requirements on the resist material aspects, thus, the resolution, LER, and sensitivity (RLS) limits cannot be resolved anymore only by an engineering approach of resist technology, and it requires fundamental studies and understanding of the interaction of light with the materials used while providing sufficient mechanical stability and patterning performance at the nanoscale targeted dimensions.

In the following tutorial, we present a brief overview of the most salient aspect of EUV photoresists. We discuss traditional and novel photoresists focusing on their patterning challenges for sub-20-nm feature size. Subsequently, we discuss those that are metal containing and their manufacturing aspects in terms of compatibility and integration. We conclude with a brief glance at which new resists lie on the horizon.

2 Resolution-LWR-sensitivity trade-off

The manufacturing requirements for the advanced technology nodes from 7 nm and below are reported in Table 1 in terms of resolution, sensitivity, and roughness.

Table 1: RLS targets for advanced technology nodes.

Tech. node name	Expected year for production (logic device)	Resolution		Sensitivity	Roughness	
		Pitch (nm)	Half-pitch (nm)	Dose (mJ/cm²)	3σ LER (nm)	3σ LWR (nm)
7 nm	2019	48	24	20	3.4	4.8
5 nm	2021	32	16	20	2.3	3.2
3 nm	2023	24	12	20	1.7	2.4

LWR and LER targets are given after resist development (ADI). LWR is given as 20% of the nominal critical dimension (CD) of the targeted feature. LER is directly linked to LWR by LWR = √2*LER [18] with the reasonable assumption that there is no correlation between LER of the left and right edge. All specifications are related to IMEC logic device roadmap.

LER is currently of particular interest, as nearly all resists are currently not able to meet the LER target [19], especially if they have to meet the resolution and sensitivity target simultaneously. Further, it seems that the LER does not continue to shrink down with the resolution scaling [20]. As local variation of the line width and the distance between lines is linked to higher failure rate for the transistor and, thus, poorer device functionality [21], it is of the foremost importance to improve the LER performances. LER is a measure of the variability of the pattern. Mathematically, LER for a line and space pattern is defined as the standard deviation from the average edge for every measurement point [16], as schematically represented in Figure 3.

Typical specification is given in 3σ line width roughness (LWR) as 20% of the nominal critical dimension (CD) of the targeted feature. LER is directly linked to LWR by LWR = √2*LER [18] with the reasonable assumption that there is no correlation between LER of the left and right edge. For example, a 22-nm L/S will require a 3σ LER below 3.1 nm. In Figure 4, the experimental relationship between exposure dose and LER is reported for the case of 22-nm dense line-space patterning. As the exposure dose decreases, the LER values get worse, roughly following a dose$^{-1/2}$ trend originated by photon shot noise [22]. It is challenging to find resists that have sensitivity and roughness both in target.

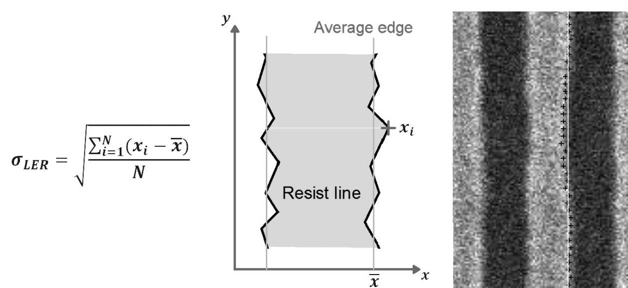

Figure 3: Left: equation of LER calculation. Right: scanning electron microscope image of a resist line pattern with LER measurements.

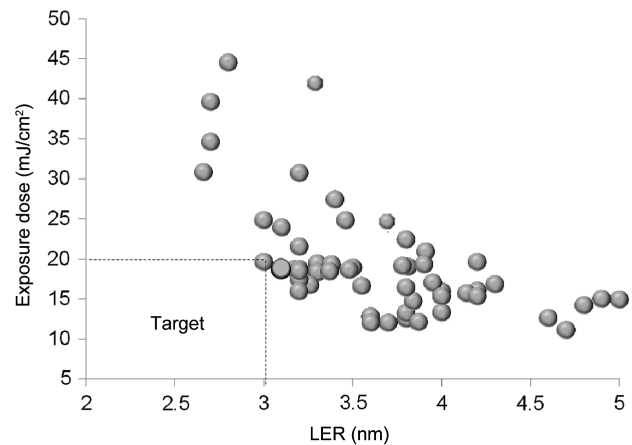

Figure 4: Exposure dose vs. LER for a 22-nm dense line-space patterning with 0.25 NA. Each point represents a different resist. It is challenging to identify a resist with LER <3.1 nm and an exposure dose below 20 mJ/cm².

3 EUV chemically amplified resist

The state-of-the-art of photosensitive materials in EUVL is the chemically amplified photoresists (CAR) [23–25] currently in use in 193 nm photolithography. These resists are a polymer blend composed of functionalized polymer chains, a photoacid generator (PAG), and a base additive. The polymer chains have hydrophilic functions that are blocked by protecting groups, rendering the polymer hydrophobic. Resins for EUV resists are mostly hydroxy styrene, acrylate, and alicyclic polymers of the kinds in use in 248 nm and 193 nm lithographic resists. The photoacid generators are also based on similar chemistries as those used on 248-nm and 193-nm lithography [26], although they are optimized to tune their sensitivity to EUV radiation. The basic workflow of patterning a silicon wafer with an EUV CAR is the same as the one used in 193-nm lithography. First, the wafer is spin coated with the resist casted in an organic solvent (i.e. PGMEA) and heated during a post-applied bake (PAB) aimed to remove

the solvent. Then, the wafer is exposed to light, and the mask pattern is transferred to the resist. In the exposed area of the resist, the PAG is decomposed into an acid [27]. Then, the wafer is heated on a hot plate for a so-called post-exposure bake (PEB). During this bake, the thermal energy is high enough to enable a deprotection reaction between the acid and the protecting groups of the polymer [28]. This reaction regenerates an acid, which acts, thus, as a catalyst, and an amplification propagation reaction occurs, with a high number (100–1000) of deprotection reaction for every acid generated during exposure. After the PEB, the polymer in the exposed area is now hydrophilic, while in the non-exposed area, it is still hydrophobic [29]. The wafer is then subjected to the development step, where, in the case of a positive tone imaging process (PTI), an aqueous solvent (TMAH 2.38%) dissolves the hydrophilic polymer chains, exposing the underlying substrate according to pattern. Later on, this pattern will be transferred to the substrate, for example, by an etching process.

In order to have a decent throughput, and because the EUV exposure tools have a limited power, the resist must have a sensitivity that is as high as possible. Nevertheless, the lower the dose, the lower the number of photon that is actually absorbed by the resist, which induces a shot noise that degrades LER [30]. Furthermore, in order to reach a tight resolution, the thickness of the photoresist must decrease in order to keep a reasonable aspect ratio (height/width) avoiding pattern collapse [31]. A typical resist film thickness range is between 30 nm and 50 nm; in the future, this will be even lower. There is, thus, less material, and the absorption of the resist must be high in order to capture the maximum number of photons. Contrary to the 193-nm case, during EUV exposure, the PAG does not directly react with the photon, as described above. The very energetic (91.6 eV) photon will ionize any molecule in the resist (mainly the polymer chains) and generates an electron. This photoelectron (~80 eV) then generates, by inelastic collision and thermalization, a bunch of secondary electrons (1–5) [32]. Finally, these secondary electrons, less energetic (~20 eV), will activate the PAG and generate the catalytic photoacid [33]. Thus, the photon shot noise (discrete light density in resist) is transformed into a secondary electron blur and then, finally, randomly generates acid molecules in the exposed polymer matrix. This acid shot noise (ASN) is also dependent on the initial concentration and repartition of PAG (chemical shot noise). During PEB, these acids will diffuse and react with the protecting groups of the polymer, which will generate in the resist zones of unprotected polymer (chemical latent image), soluble in the developer [34]. Hence, the acid diffusion is needed during PEB to make the amplification reaction possible. Nevertheless, the acid diffusion is also limiting resolution, as the acid diffusion length needs to be significantly lower than the critical dimension (CD) printed in order to ensure steep edges of the chemical latent image. In order to get a better chemical contrast, a base component is added to quench the acid [35]. This quencher is uniformly distributed in the resist and will, thus, have a strong quenching effect in the non-exposed region where the base/acid ratio is high, ensuring that amplification reaction will not take place. Conversely, in the exposed region, the acid concentration will be lowered by this quenching, which has a negative effect on the sensitivity of the resist [36]. Aside from these classical positive tone chemically amplified resists, negative tone development (NTD) is being developed. For these CA resists, the development step is done with an organic solvent, and it is the unexposed resist, hydrophobic, that is dissolved. The exposed hydrophilic resist remains, providing the negative of the mask pattern. Another negative tone imaging (NTI) approach are the negative tone resists: here, the difference resides in the resist formulation where the hydrophilic functions of the polymer are not covered by protecting groups, and more importantly, crosslinker molecules are added to the blend. These molecules will be activated whether directly during exposure, or by the photoacid in the exposed region, and will chemically bond the different polymer chains by crosslinking during PEB. The exposed resist will, thus, form an insoluble polymer network. The development step is then processed with aqueous solvent, removing the non-exposed regions. It should be noted that negative tone resist with direct photo activation of the crosslinker are commonly used in I-line lithography. NTI approach is interesting for EUV lithography as better results in terms of LER have been obtained [37], probably due to the difference in development mechanism or due to the different number of involved photons between negative and positive tone. Nevertheless, both types still rely on a chemical amplification mechanism and are, thus, based on the diffusion of an acid.

Recently, new further efforts have been done on the CAR resist front in order to accomplish the RLS targets. As the dimension of the polymer chains of the resist are getting closer to the critical dimension targeted, reducing the size of the building blocks that needs to be removed during development should potentially help to reduce LER. The investigation of calixarene-derived molecular glass [38], as alternatives to polymeric, or the use of fullerenes [39], as resist material, are attractive for their small molecular size compared to traditional CAR. A new series of novel organic-inorganic (hybrid) resist systems has

been also developed, composed of a hafnium or zirconium oxide nanoparticle core and an organic methacrylate shell, they combine small size and high sensitivity in extreme ultraviolet light and excellent etch resistance with oxygen plasma and fluorinated etch gases compared to organic materials [40].

4 Toward novel EUV resists

Today, a possible viable path to overcome the RLS trade-off in EUV lithography is the identification of alternative resists (i) with novel solubility switching mechanisms able to suppress the existing blur effects and (ii) with better EUV light absorption to capture more productive photons and offer better sensitivity.

In order to minimize the resist blur effect, the solubility switch should happen within a short distance from the ionization point where the photoelectrons are generated with a short mean free path of the secondary electrons. Such a switching mechanism would suggest a mechanism without chemical amplification, i.e. non-chemically amplified resists (NCAR).

Novel resist design schemes have been reported as positive tone resist strategy based on de-polymerization or cleavage of a densely crosslinked organic resin. By crosslinking, the resist forms a dense three-dimensional network, and the mechanical strength and adhesion of the resist are greatly improved compared to structures of linear polymer, which are only held together by cohesive energy between chains. The improved mechanical strength should improve pattern collapse performance [23]. A complete new approach based on molecular layer deposition has been recently demonstrated as potential new method for synthetizing new photoresists with the advantages of precise control over organic film and homogenous composition [41]. An extension for CA resist that is currently explored addresses the reduction of the size of the polymer chains [42, 43]. Pushing this idea to its limits, the polymer can be reduced to a single component molecular resist, each molecule containing the needed functions linked together [44]. Notably, Cornell University has developed an amorphous molecular glass resist, with promising results in terms of resolution [45]. Birmingham University has also developed molecular resists with even smaller dimensions, based on fullerene derivatives. These negative tone resist relies on crosslinking of epoxy [46]. The latest advances with these materials use a molecule called xMT (not fullerene-based anymore), and it has shown resolution capability up to 14 nm [47]. A better understanding of the mechanism and performances is still needed.

As the number of EUV photons reaching the wafer is limited, it is very important that a majority of them are captured within their travel through the very thin photoresist film. The absorbance of EUV radiation is relatively high for most of the materials; nevertheless, as the photoresist film is only around 30–50-nm thick, the majority of the photons cross the resist to reach the substrate [48]. Therefore, increasing absorbance and the conversion of photons into secondary electron are important paths to improve resist sensitivity. The molar absorbance of different atoms is well known [49], and adding atoms with high-absorbing cross sections into the resist composition allows to collect more photons. Fluoride-containing resists and PAG have been explored. Therefore, another option is to add to the polymer blend another component, called sensitizer, which aims to enhance the EUV absorbance. The influence of such sensitizer on the sensitivity has been recently proven [50], but the impact of such a sensitizer on dissolution and LER should be further assessed.

Another interesting concept design on non-chemically amplified resist is based on a negative tone resist strategy where metal-oxide molecules crosslink into a network by EUV exposure and bake [51]. An introduction to metal-containing resist (MCR) is given in the next paragraph.

5 Metal-containing resist

Strong interest has recently developed among the researchers in the use of metals in extreme ultraviolet lithography photoresists [52–55] aiming to improve the resist sensitivity by increasing the EUV absorbance compared to traditional organic resist, thus, capturing more EUV photons and making a more productive use of the secondary electrons. If the metal is appropriately selected, other benefits can be obtained from its introduction into the resist formulation. For instance, organic thin films used in EUV lithography can significantly limit the ability to transfer the pattern to the substrate during the etch steps that follow exposure. To obviate the need for a hard-mask layer and the associated increase in the process costs, the improvement of the resist etch resistance using a MCR can be a reasonable approach. Furthermore, because of the high etch resistance due to the metal content into the film, a thinner film thickness can be applied (as low as 20 nm) with potential benefits on the line collapse performance as a consequence. Challenges for a MCR are to keep a high-performing switching

solubility mechanism, to maintain patterning fidelity and to mitigate shot noise with a better trade-off between sensitivity and LER compared to CARs. In this respect, several patterning attempts on ASML NXE3300 full-field exposure tool have been recently reported using MCRs [56–58]. The obtained results give indication that, for instance, adding a metal into a CAR formulation does not always directly lead to an increase in the electron response of the resist when exposed under the EUV light. Furthermore, a MCR does not necessarily show good EUV lithographic performance, suggesting that only if the chemistry is right, the benefits from a metal system can be attained. A good example is the metal-oxide resist developed by Inpria Corporation that will be discussed in the next paragraph.

6 Metal-oxide resist (Inpria resist case)

The MCR developed by Inpria consists of small clusters of metal oxide/organic particles without the addition of any other molecular species, contrary to the CAR (i.e. PAG or quencher). Such a MCR has shown excellent lithographic performance on par with CARs. Top-down images on 13-nm dense line-space patterning for both organic CAR and metal oxide-based resists are reported in Figure 5. Furthermore, Inpria metal oxide resist (MOR) offers high etch resistance because of their intrinsic properties [59], and they can, therefore, serve as a useful alternative to conventional organic films with the advantage of being used very thin (below 20-nm film thickness) minimizing the risk of pattern collapse if compared to an equivalent CAR process with its optimized film thickness. An example of benefit on pattern collapse margin is shown in Figure 6 [60].

Inpria metal oxide resist has an etch rate that is about 57 times lower than that of an organic resist (using an oxygen-based chemistry), which enables a simplified bilayer system for the direct exposure of the metal oxide resist on top of a sacrificial carbon layer, eliminating the need for the intermediate spin-on-glass hardmask present in the patterning stack when using a CAR [61].

The Inpria metal oxide resist has been demonstrated to be a valid alternative to traditional organic CAR in EUV lithography with high patterning resolution, better line collapse margin, and higher etch resistance than CAR, Nevertheless, the benefits from high EUV absorbance (~18 μm^{-1}) and non-diffusion system have to be proven as the current barrier of the RLS trade-off is not broken yet, and LER still remains far from the targets reported in Table 1. The LER reduction, together with the manufacturing compatibility for high-volume manufacturing (HVM) purpose, is the next challenge for this MCR.

7 Metal-containing resist challenges in a manufacturing environment

MCRs have to demonstrate breakthrough litho performances to compete with traditional organic materials because the introduction of MCRs in the line of an HVM

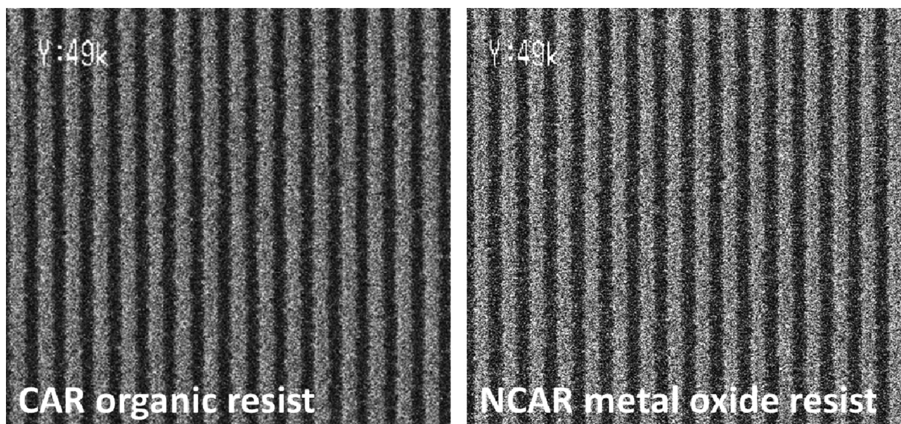

Figure 5: Top-down images on scanning electron microscope Hitachi CG5000 taken with rectangular scan 150 K×49 K magnification on a 13-nm half-pitch dense line-space pattern. Left: advanced chemically amplified resist 25-nm thick and exposed at 35 mJ/cm^2. Right: metal oxide-based resist developed by Inpria Corporation, 18-nm thick and exposed at 38 mJ/cm^2. Both resists were exposed at the optimum process conditions on ASML NXE3300 full-field exposure scanner at IMEC, Belgium. Both CAR and MOR gave a comparable LWR equal to 3.9 nm and 3.8 nm, respectively.

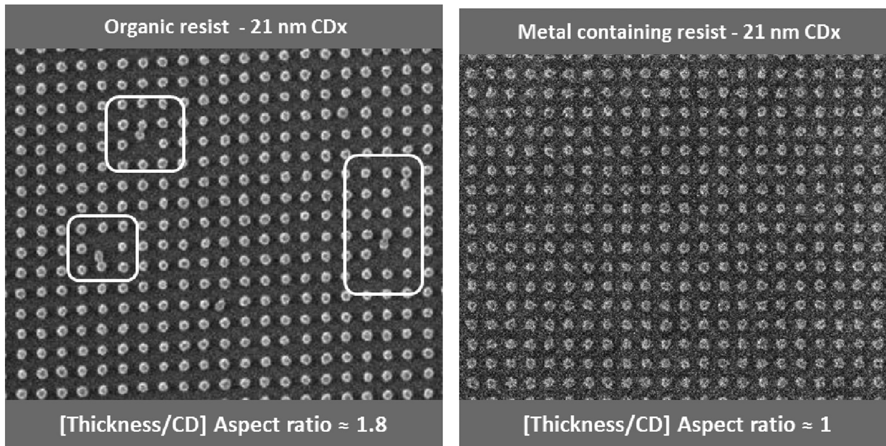

Figure 6: A 42-nm pitch dense pillar pattern. Left: a CAR with approximately 1.8 as FT/CD aspect ratio shows pattern collapse. Right: a metal oxide resist developed by Inpria Corporation with approximately 1.0 as FT/CD aspect ratio does not show pattern collapse.

device flow opens new scenarios about the management of wafers and tools at contamination and process level, due to the risk of cross metal contamination and outgassing metal species when exposed on EUV tools, risks that are inexistent with traditional organic material. As a MCR intentionally contains one or more metal species, it is critical to assess the risk of metal transport between wafers during the coat process. The primary focus is on the metal intentionally added into the formulation. Transmission X-ray fluorescence spectroscopy (TXRF) is typically used to detect trace metals on silicon wafers, with detection limits on the order of 1E10 atoms/cm^2 common for cross-contamination specifications. In some cases, the metal species can have a partial conflict with silicon, so detection limits can be somewhat higher for some metal species on a silicon background. A typical case is the Sn species where the detection limit on TXRF can reach ~1E12 t/cm^2. To get additional perspective, vapor phase decomposition (VPD) is used in combination with ICP-MS or TXRF tool, which has a better detection limit of about ~1E8 atoms/cm^2, at the expense of reduced spatial resolution.

Experiments conducted on two different classes of MCRs have shown no risk of cross-contamination at tool level (litho and etch), with metal concentration level below the specification limit of 1E10 atoms/cm^2 [56, 62, 63].

Furthermore, in the EUV scanner vacuum environment, hydrogen gas (H_2) is present, and with EUV photons, it can lead to atomic H or radical H* that can interact with the metal species of MCR to form metallic hydrides (Mx-Hy). Mx-Hy deposition on EUV mirror surfaces presents a serious risk to optics lifetime; therefore, it is important to understand if the metal species present in MCR can lead to the metal hydride formation when in contact with an H_2 environment.

Currently, all the alternative resists that contain elements different from C, H, O, N, S, F need ASML to grant a waiver for exposure on the NXE EUV scanner tools [64]. Even though the results from cross-contamination tests look promising and several waivers have been granted by ASML for specific metal species, cross metal contamination and metal hydrides risks have to be assessed at a larger scale for the HVM qualification.

In addition, ASML has recently announced the introduction of a dynamic gas lock (DGL) membrane in their EUV scanner, to release the contamination requirement at exposure level. The DGL membrane is an 85% EUV-transparent membrane that seals the wafer level from the optical parts of the scanner, effectively suppressing the

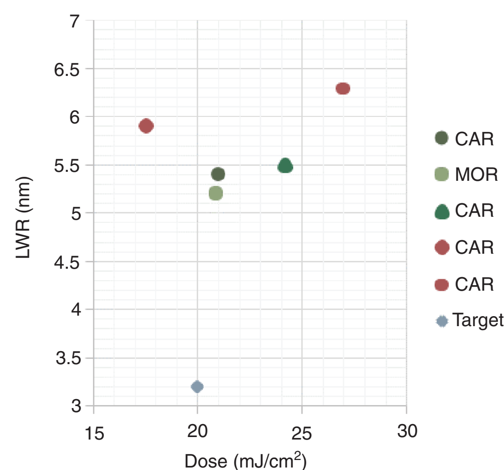

Figure 7: A 16-nm half-pitch dense line-space pattern, 0.33NA, and manufacturable dipole illumination. LWR is plotted with the corresponding exposure dose for five advanced EUV resists. The resists are able to work under the low-exposure dose regime, but the LWR is quite far from the specification of 3.2 nm.

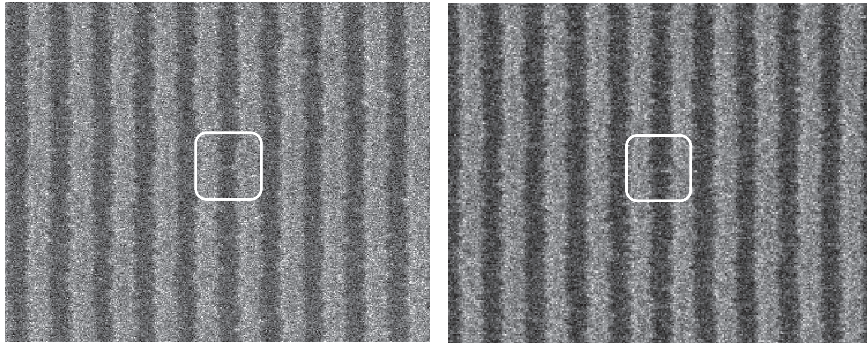

Figure 8: A 16-nm half-pitch dense line-space pattern. CAR on the left, MOR on the right. Both resists shows nanobridges. Root cause of such an issue is currently under investigation. Nanobridge defectivity is the major issue nowadays for high-sensitivity EUV resists that need to satisfy HVM requirements.

risk of contamination from resist outgas [65]. Nevertheless, the cost of a reduced power reaching the wafer and cross metal contamination risks have to be assessed.

8 State-of-the-art of high-sensitivity EUV resists

The results of a recent exploration aiming to assess the high-sensitivity EUV resists with manufacturable requirements have been reported out [63]. This evaluation has been conducted on 16-nm half-pitch dense line-space pattern, which represents the critical feature size for BEOL metal layer of a 5-nm technology node logic device.

The results in terms of exposure dose and LWR for the best performing EUV resists are reported in Figure 7, where both CAR and metal oxide resists are included.

Although resists can reach high sensitivity (~20 mJ/cm^2), the LWR target of 3.2 nm is not achieved. Furthermore, the high-sensitivity resists show defectivity at nanoscale, and this problem represents, nowadays, the most critical issue to be tackled for such a class of EUV resists. An example of nanodefectivity is reported in Figure 8.

9 Novel EUV resists lie on the horizon

The RLS trade-off is still a diehard, and a breakthrough in this respect is needed. The development of novel high-absorbing CARs with a well-controlled low-acid diffusion length is on the way; however, the early stage exploration is focused, nowadays, on the development of molecular resists rather than polymeric. Metal oxide cluster resist is currently a good candidate to deliver the needed breakthrough. Furthermore, some research groups rely on the use of metal species like antimony and metal-organic framework (MOF) structures that can provide novel mechanisms of EUV light-matter interaction and a digital solubility switching mechanism [66, 67]. Other research groups rely on molecular resist metal-free and no post-exposure bake based on a novel type of resist chemistry known as a multi-trigger resist system [68]. An emerging path is the combination of current and novel resists with high-NA scanner that should deliver more contrast, allowing for a smaller exposure dose at the same resolution or even a higher exposure dose at good throughput [69, 70].

Efforts are still needed from all the stakeholders to make EUVL HVM possible and cost-effective as soon as possible.

Acknowledgments: The authors wish to thank Dr. Jan van Schoot from ASML for the valuable discussions.

References

[1] IBM Media Relation, ‘IBM Research Alliance Produces Industry’s First 7nm Node Test Chips’, Press Release on 09-Jul-2015, https://www-03.ibm.com/press/us/en/pressrelease/47301.wss.
[2] V. Y. Banine, Inaugural lecture at Eindhoven University of Technology, EUV Lithography: Historical perspective and road ahead, 19-Sept-2014.
[3] J. Hecht, ‘Photonic frontiers: EUV lithography: EUV lithography has yet to find its way into the fab’, LaserFocusWorld, (January 5, 2013). Available: http://www.laserfocusworld.com/articles/print/volume-49/issue-05/features/photonic-frontiers--euv-lithography--euv-lithography-has-yet-to-.html.
[4] I. Fomenkov, ‘Status and outlook of LPP light sources for HVM EUVL,’ in EUVL Workshop 2015. Available: http://euvlitho.com/2015/P3.pdf.

[5] T. Itani, P. Gargini, K. Ronse and P. Naulleau, ‘Closing Address’, EUVL symposium 2016, Hiroshima, Japan.
[6] N. Mojarad, M. Hojeij, L. Wang, J. Gobrecht and Y. Ekinci, Nanoscale 7, 4031–4037 (2015).
[7] C. Mack, Fundamental Principles of Optical Lithography: The Science of Microfabrication (John Wiley & Sons, Chichester, UK, 2011).
[8] S. J. Moss and A. Ledwith, Chemistry of the Semiconductor Industry (Springer, Dordrecht, Netherlands, 1989).
[9] T. Wallow, ‘EUV resists considered as materials for optics,’ IEUVI TWG meeting 27-2-2011.
[10] J. W. Thackeray, Proc. SPIE 7972, 797204 (April 15, 2011); doi:10.1117/12.882958.
[11] J. van Schoot, K. van Ingen Schenau, C. Valentin and S. Migura, Proc. SPIE 9422, 94221F (March 16, 2015); doi:10.1117/12.2087502.
[12] B. Kneer, S. Migura, W. Kaiser, J. T. Neumann and J. van Schoot, Proc. SPIE 9422, 94221G (March 16, 2015); doi:10.1117/12.2175488.
[13] K. Yoshimoto, P. Stoykovich, H. B. Cao, J. J. de Pablo, P. F. Nealey and W. J. Drugan, J. Appl. Phys. 96, 1857 (2004).
[14] H. B. Cao, P. F. Nealey and W.-D. Domke, J. Vac. Sci. Technol. B 18, 3303 (2000).
[15] K. Petrillo, G. Huang, D. Ashworth, J. Georger, L. Ren, et al., Proc. SPIE, 7969, id. 796913 (2011).
[16] A. Vaglio Pret, Modelling and Experimental Evaluation of (Post) lithography Process Contributions to Pattern Roughness, PhD thesis, (KU Leuven, 2012).
[17] J. M. Hutchinson, Proc. SPIE 3331, pp.531–536, (June 5, 1998); doi: 10.1117/12.309612.
[18] T. Marschner, A. Lee, S. Fuchs, L. Völkel and C. Stief, Proc. SPIE 5375, 479 (2004).
[19] P. P. Naulleau, D. Niakoula and G. Zhang, J. Vac. Sci. Technol. B 26, 1289–1293 (2008).
[20] D. Van Steenwinckel, J. H. Lammers, T. Koehler, R. L. Brainard and P. Trefonas, J. Vac. Sci. Technol. B 24, 316–320 (2006).
[21] A. V. Pret, P. Poliakov, R. Gronheid, P. Blomme, M. M. Corbalan, et al., Microelectron. Eng. 98, 24–28 (2012).
[22] R. Brainard, in ‘EUV Lithography’, Ed. by V. Bakshi (SPIE Press, Bellingham, Washington USA, 2009) pp. 383–448. DOI: 10.1117/3.769214.ch8.
[23] R. A. Lawson, J. Cheng, A. Cheshmehkani, L. M. Tolbert and C. L. Henderson, Proc. SPIE 8682, 868221-2 (2013).
[24] W. Wu, K. Nuzhdin, M. Vyushkova, I. Janik and D. Bartels, J. Phys. Chem B 116, 6215–6224 (2012).
[25] B. Wu and A. Kumar, J. Vac. Sci. Technol. B 25, 1743–1761 (2007).
[26] T. Kozawa and S. Tagawa, J. Photopolym. Sci. Technol. 24, 137–142 (2011).
[27] K. Kemp and S. Wurm, Comptes Rendus Physique 7, 875–886 (2006).
[28] A. Erdmann, T. Fuehner, P. Evanschitzky, V. Agudelo, C. Freund, et al., Microelectron. Eng. 132, 21–34 (2015).
[29] H. Ito, IBM J. Res. Dev. 41, 69–80 (1997).
[30] J. J. Biafore, M. D. Smith, C. A. Mack, J. W. Thackeray, R. Gronheid, et al., Proc. SPIE 7273, 727343 (10 pp.) (2009).
[31] K. Yoshimoto, C. Higgins, A. Raghunathan, J. G. Hartley, D. L. Goldfarb, et al., Proc. SPIE 7972, 79720K (12 pp.) (2011).
[32] T. Kozawa and S. Tagawa, J. Vac. Sci. Technol. B 25, 2481–2485 (2007).
[33] T. Kozawa and S. Tagawa, Jpn. J. Appl. Phys. 49, 030001 (2010).
[34] T. Itani and T. Kozawa, Jpn. J. Appl. Phys. 52, 010002 (2013).
[35] S. Nagahara, Y. Lei, W. J. Poppe, A. Neureuther, Y. Kono, et al., Proc. SPIE 5753, 338–349 (2005).
[36] T. Kozawa, S. Tagawa, J. J. Santillan and T. Itani, J. Photopolym. Sci. Technol. 21, 421–427 (2008).
[37] T. Fujimori, T. Tsuchihashi and T. Itani, J. Photopolym. Sci. Technol. 28, 485–488 (2015).
[38] H. Kudo and S. Matsubara, in ‘International Workshop on EUV Lithography’, 2013.
[39] A. Frommhold, D. X. Yang, A. Mc Clelland, X. Xued, R. E. Palmera, et al., Proc. SPIE 8682, 86820Q-1 (2013).
[40] M. Trikeriotis, M. Krysak, Y. Sook Chung, C. Ouyang, B. Cardineau, et al., Proc. SPIE 8322, 83220U-1 (2012).
[41] H. Zhou and S. F. Bent, Proc. SPIE 8682, 86820U-1 (2013).
[42] H. Tsubaki, K. Yamashita, H. Takahashi, D. Kawamura and T. Itani, Proc. SPIE 7273, 72733S (10 pp.) (2009).
[43] G. P. Patsis, E. Gogolides and K. Van Werden, Jpn. J. Appl. Phys. Part 1-Regular Papers Brief Communications & Review Papers 44, 6341–6348 (2005).
[44] C. L. Henderson, ‘Molecular Resists for EUV Lithography: A Progress Report,’ Georgia Institute of Technology, Sematech, 2008. Available: http://www.sematech.org/meetings/archives/litho/8352/pres/D1_EUV_P04_Henderson.pdf.
[45] A. De Silva, N. M. Felix and C. K. Ober, Adv. Mater. 20, 3355–3361 (2008).
[46] A. Frommhold, D. Yang, A. McClelland, X. Xue, Y. Ekinci, et al., J. Micro-Nanolithogr. MEMS MOEMS 12, 033010 (2013).
[47] A. Frommhold, A. McClelland, D. Yang, R. E. Palmer, J. Roth, et al., Proc. SPIE 9425, 942504 (8 pp.) (2015).
[48] D. F. Kyser, N. K. Eib and N. W. M. Ritchie, J. Micro-Nanolithogr. MEMS MOEMS 15, 033507 (2016).
[49] B. L. Henke, E. M. Gullikson and J. C. Davis, At Data Nucl. Data T. 54, 181–342 (1993).
[50] V.-K. M. Kuppuswamy, V. Constantoudis, E. Gogolides, A. V. Pret and R. Gronheid, J. Micro-Nanolithogr. MEMS MOEMS 12, 023003 (2013).
[51] A. Grenville, ‘Advances in Directly Patternable Metal Oxides for EUV Resist’, EUVL Symposium 2013, Toyama, Japan (2013). Available: http://euvlsymposium.lbl.gov/pdf/2013/pres/S3-3_AGrenville.pdf.
[52] M. Neisser, K. Cho and K. Petrillo, J. Photopolym. Sci. Technol. 25, 87–94 (2012).
[53] B. Cardineau, J. Passarelli, M Sortland, R. Del Re, W. Tear, et al., EUVL Symposium, 2013.
[54] B. Cardineau, M. Krysak, M. Trikeriotis, E. P. Giannelis, C. K. Ober, et al., Proc. SPIE 8322, 83220V-1 (2012).
[55] S. Chakrabarty, C. Ouyang, M. Krysak, M. Trikeriotis, K. Cho, et al., Proc. SPIE 8679, 867906-8 (2013).
[56] D. De Simone, S. Sayan, S. Dei, I. Pollentier, Y. Kuwahara, et al., Proc. SPIE Extreme Ultraviolet (EUV) Lithography VII, 9776, 977606 (2016).
[57] D. De Simone, M. Ming, F. Lazzarino and G. Vandenberghe, J. Photopolym. Sci. Technol, 29, 501 (2016).
[58] D. De Simone, I. Pollentier and G. Vandenberghe, J. Photopolym. Sci. Technol. 28, 507 (2015).
[59] Y. Kuo, in ‘Proc. 11th Int’l Symp. Plasma Process’, pp. 536–540, 1996.
[60] D. De Simone, M. Ming and G. Vandenberghe, ‘Novel metal-oxide photoresist materials for extreme UV lithography’, SPIE

Newsroom (July 1, 2016); doi:10.1117/2.1201606.006534. Available: http://spie.org/newsroom/6534-novel-metal-oxide-photoresist-materials-for-extreme-uv-lithography.
[61] D. De Simone, M. Ming, M. Kocsis, P. De Schepper, F. Lazzarino, et al., Proc. SPIE 9776, 97760B (2016).
[62] A. Grenville, J. T. Anderson, B. L. Clark, P. De Schepper, J. Edson, et al., Proc. SPIE 9425, 94250S-1 (2015).
[63] D. De Simone, Y. Vesters, A. Shehzad, G. Vandenberghe, P. Foubert, et al., Proc. SPIE 10143, 101430R (March 24, 2017); doi:10.1117/12.2258220.
[64] G. Rispens, 'Status update on outgassing of alternative resists', Resist TWG, February 21 2016.
[65] M. van de Kerkhof, H. Jasper, L. Levasier, R. Peeters, R. van Es, et al., Proc. SPIE 10143, 101430D (2017).
[66] K. Kasahara, H. Xu, V. Kosma, J. Odent, E. P. Giannelis, et al., Proc. SPIE 10143, 1014308 (March 24, 2017); doi:10.1117/12.2258187.
[67] M. Murphy, A. Narasimhan, S. Grzeskowiak, J. Sitterly, P. Schuler, et al., Proc. SPIE 10143, 1014307 (March 31, 2017); doi:10.1117/12.2258119.
[68] C. Popescu, A. Frommhold, A. L. McClelland, J. Roth, Y. Ekinci, et al., Proc. SPIE 10143, 101430V (March 24, 2017); doi:10.1117/12.2258098.
[69] J. van Schoot et al., 'EUV roadmap extension by higher Numerical Aperture', EUVL conference 2016, Hiroshima, Japan.
[70] E. van Setten et al., 'EUV high NA anamorphic imaging', EUVL conference 2016, Hiroshima, Japan.

Danilo De Simone
Advanced Patterning Department, IMEC
Kapeldreef 75, Heverlee B-3001, Belgium
danilo.desimone@imec.be

Danilo De Simone received his MS degree in Chemistry from the University of Palermo, and in 2000, he joined STMicroelectronics in Italy. Until 2007, he led the development of lithographic materials for 90-nm and 65-nm NOR flash devices and covered the role of assignee at STM Crolles2 R&D Fab in France and STM Singapore fab working on multiple R&D and production projects. In 2008, he moved to Numonyx taking the ownership to develop 32-nm double patterning modules for phase-change memory devices. In 2011, after Numonyx was acquired by Micron Technology, he worked to introduce in HVM 45-nm PCM devices and to support the lithographic development of novel magnetic devices. In 2013, he joined IMEC in Belgium leading the exploration of photomaterials for EUV lithography.

Yannick Vesters
Advanced Patterning Department, IMEC
Kapeldreef 75, Heverlee B-3001, Belgium; and
Department of Chemistry, KU Leuven
Celestijnenlaan 200F, Heverlee B-3001
Belgium

Yannick Vesters received his BS and MS degrees in Chemical Engineering and Material Science from the University of Louvain-la-Neuve, Belgium. During his MS, he spent 1 year at the Simon Bolivar University in Venezuela. He worked as an engineer for 2 years before starting his PhD at the University of Leuven, Belgium. He is currently performing his PhD research on the improvement of the lithographic performances of photoresists for EUV lithography at IMEC. He focuses on the understanding of patterning mechanism and on novel photoresist materials.

Geert Vandenberghe
Advanced Patterning Department, IMEC
Kapeldreef 75, Heverlee B-3001, Belgium

Geert Vandenberghe PhD has been at IMEC for over 20 years. He joined IMEC's Lithography Department in 1995 where he has been working in multiple areas such as resists, imaging, resolution-enhancement techniques, and on various wavelengths ranging from 248 nm to 13.5 nm, all in the framework on IMEC's Advanced Lithography Research Program. Currently, he is managing the Exploratory Patterning R&D activities, including EUV lithography and Directed Self-Assembly. Geert Vandenberghe received his Master of Science and PhD degrees from the Katholieke Universiteit of Leuven in Belgium.